J Paleolimnol (2014) 51:223–240
DOI 10.1007/s10933-013-9721-y

ORIGINAL PAPER

Abrupt deglaciation on the northeastern Tibetan Plateau: evidence from Lake Qinghai

Xiuju Liu · Steven M. Colman · Erik T. Brown · Andrew C. G. Henderson · Josef P. Werne · Jonathan A. Holmes

Received: 22 March 2012 / Accepted: 26 April 2013 / Published online: 3 August 2013

Abstract We inferred the climate history for Central Asia over the past 20,000 years, using sediments from core QH07, taken in the southeastern basin of Lake Qinghai, which lies at the northeastern margin of the Tibetan Plateau. Results from multiple environmental indicators are internally consistent and yield a clear late Pleistocene and Holocene climate record. Carbonate content and total organic carbon (TOC) in Lake Qinghai sediments are interpreted as indicators of the strength of the Asian summer monsoon. Warm and wet intervals, associated with increased monsoon strength, are indicated by increased carbonate and TOC content. During the glacial period (~20,000 to ~14,600 cal year BP), summer monsoon intensity remained low and relatively constant at Lake Qinghai, suggesting cool, dry, and relatively stable climate conditions. The inferred stable, cold, arid environment of the glacial maximum seems to persist through the Younger Dryas time period, and little or no evidence of a warm interval correlative with the Bølling–Allerød is found in the QH07 record. The transition between the late Pleistocene and the Holocene, about 11,500 cal year BP, was abrupt, more so than indicated by speleothems in eastern China. The Holocene

Electronic supplementary material The online version of this article (doi:10.1007/s10933-013-9721-y) contains supplementary material, which is available to authorized users.

X. Liu (✉) · S. M. Colman · E. T. Brown · J. P. Werne
Large Lakes Observatory, University of Minnesota, Duluth, Duluth, MN 55812, USA
e-mail: liuxx669@umn.edu

S. M. Colman
e-mail: scolman@d.umn.edu

E. T. Brown
e-mail: etbrown@d.umn.edu

J. P. Werne
e-mail: jwerne@d.umn.edu

X. Liu
Department of Earth Sciences, University of Minnesota, Minneapolis, MN 55455, USA

E. T. Brown
Department of Geological Sciences, University of Minnesota, Duluth, Duluth, MN 55812, USA

A. C. G. Henderson
School of Geography, Politics and Sociology, Newcastle University, Newcastle upon Tyne NE1 7RU, UK
e-mail: andrew.henderson@ncl.ac.uk

J. P. Werne
Department of Chemistry and Biochemistry, University of Minnesota, Duluth, Duluth, MN 55812, USA

Present Address:
J. P. Werne
Department of Geology and Planetary Science, University of Pittsburgh, 4107 O'Hara St, SRCC 505, Pittsburgh, PA 15260, USA

J. A. Holmes
Environmental Change Research Centre, University College London, London WC1E 6BT, UK
e-mail: j.holmes@ucl.ac.uk

(~11,500 cal year BP to present) was a time of enhanced summer monsoon strength and greater variability, indicating relatively wetter but more unstable climatic conditions than those of the late Pleistocene. The warmest, wettest part of the Holocene, marked by increased organic matter and carbonate contents, occurred from ~11,500 to ~9,000 cal year BP, consistent with maximum summer insolation contrast between 30°N and 15°N. A gradual reduction in precipitation (weakened summer monsoon) is inferred from decreased carbonate content through the course of the Holocene. We propose that changes in the contrast of summer insolation between 30°N and 15°N are the primary control on the Asian monsoon system over glacial/interglacial time scales. Secondary influences may include regional and global albedo changes attributable to ice-cover and vegetation shifts and sea level changes (distance from moisture source in Pacific Ocean). The abruptness of the change at the beginning of the Holocene, combined with an increase in variability, suggest a threshold for the arrival of monsoonal rainfall at the northeastern edge of the Tibetan Plateau.

Keywords Lake Qinghai · Tibetan Plateau · Asian monsoon · Geochemistry · Abrupt deglaciation

Introduction

The Tibetan Plateau has long been considered a major control on monsoonal circulation over Asia, as suggested by the contrast between climate models that include and exclude the topography of the plateau (Kutzbach et al. 1989). The classical explanation of the impact of enhanced heating of the atmosphere over Tibet on the Asian monsoons during spring and summer may be an oversimplification. The dynamics of the Asian monsoon may also be affected by the barrier posed by the plateau in the path of the subtropical jet stream (Molnar et al. 2010). Another factor may be orographic insulation, by which the height of the Himalayas at the south margin of the plateau blocks moisture exchange between the tropics and mid-latitudes (Boos and Kuang 2010; Molnar et al. 2010). Whatever the exact mechanisms involved, the presence of the Tibetan Plateau clearly affects the distribution of precipitation in southern and eastern Asia.

Oxygen isotopes of cave speleothems within the monsoonal region have been widely used as an indicator of the intensity of the East Asian monsoon (Wang et al. 2001; Yuan et al. 2004). These cave records generally reveal a relatively weak East Asian monsoon during the glacial period and a strong monsoon in the Holocene, following changes in the Northern Hemisphere summer insolation on the orbital timescale. Millennial-scale climate events, such as those correlated with the Bølling–Allerød oscillation, the Younger Dryas event, and the 8.2 ka cooling event, are clearly recorded in these speleothems. However, numerical climate simulations with an embedded oxygen-isotope model suggest that changes in oxygen isotopic compositions in the Chinese caves (including Hulu and Dongge) reflect changes in the intensity of the South Asian rather than East Asian monsoon precipitation (Pausata et al. 2011).

Lake Qinghai (Fig. 1), as a consequence of its unique geographical setting on the Tibetan Plateau, is sensitive to environmental and climatic changes and thus well-suited for study of the Asian monsoon and the Westerlies at various time scales (Colman et al. 2007; Henderson and Holmes 2009; Henderson et al. 2010; An et al. 2012). However, only a handful of studies (Lister et al. 1991; Shen et al. 2005) have used multiple biogeochemical analyses of the sediments of Lake Qinghai to interpret regional climatic and environmental changes. These studies have suggested a cold-dry glacial time, a moist early Holocene during the insolation and monsoon maximum, followed by a drying trend during the middle and late Holocene, but most of these studies had relatively limited chronological constraints. Radiocarbon dating of Lake Qinghai sediment is difficult because macro-organic matter is scarce and because of carbon reservoir effects in the lake (An et al. 2012). Moreover, the climate pattern reconstructed from the pollen record in Hurleg Lake, 300 km west of Lake Qinghai, appears to be opposite to the climate pattern inferred at Lake Qinghai (Zhao et al. 2007). A few studies have also attempted to reconstruct the lake-level history of Lake Qinghai from core data (Lister et al. 1991; Yu and Zhang 2008). Lister et al. (1991) suggest substantial lake-level rises during the periods approximately 10,200–9,800, 9,500–8,500, 8,300–7,200 cal year BP and probable decreased levels during the intervening intervals. However, these lake-level inferences are not entirely compatible with recent dating studies

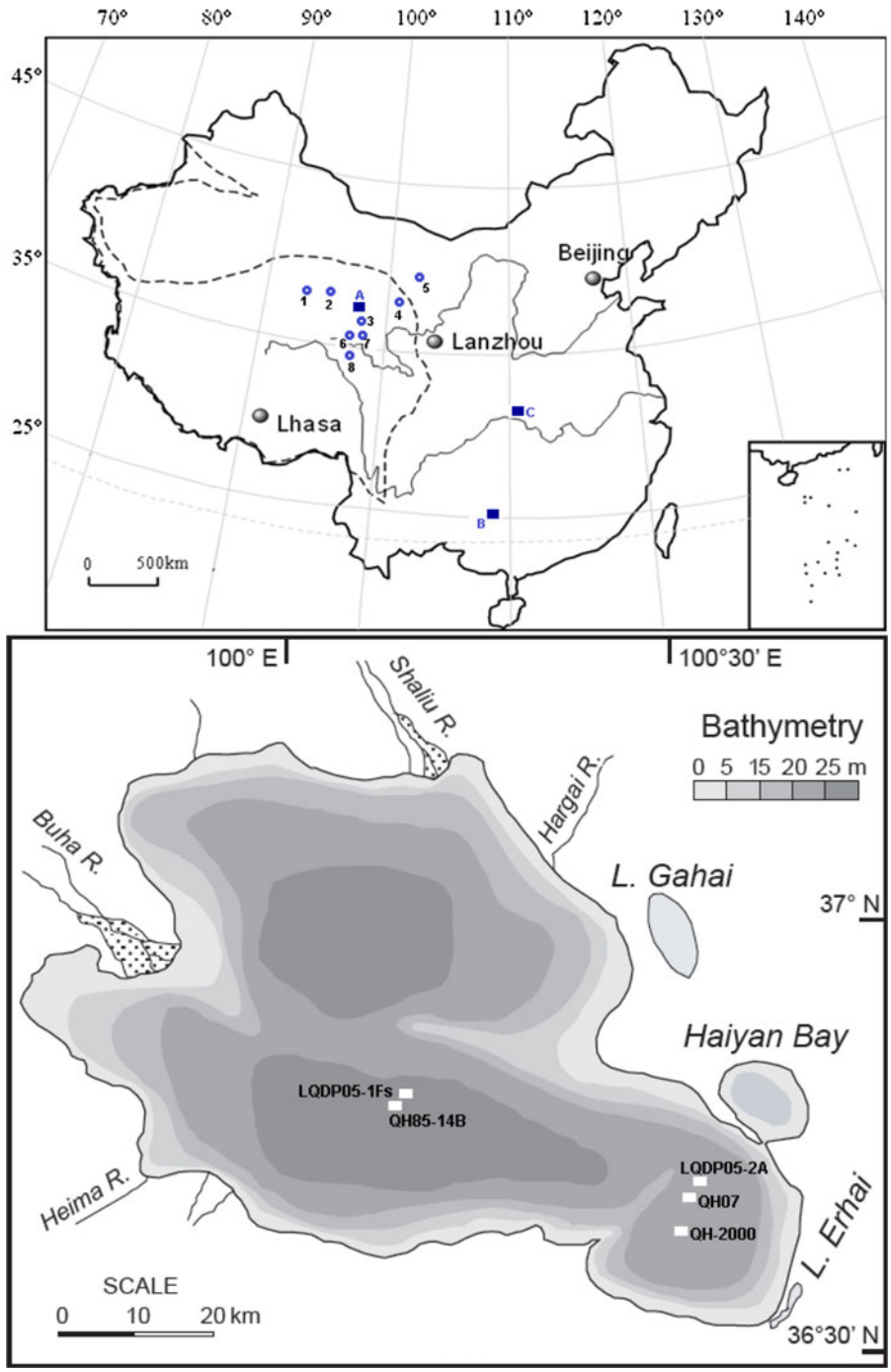

Fig. 1 Map of China showing the setting of Lake Qinghai on the Tibetan Plateau (the *broken line* indicates the area of the Tibetan Plateau), Chinese caves, and the sites of other regional lake records discussed in the text (*A* Lake Qinghai; *B* Dongge Cave, Yuan et al. 2004; *C* Sanbao Cave, Wang et al. 2008; *1* Hurleg Lake, Zhao et al. 2007; *2* Chaka Salt Lake, Liu et al. 2008; *3* Dalianhai Lake, Chen et al. 2012; *4* Shiyang River drainage basin, Li et al. 2012; *5* Ulan Buh Desert region, Zhao et al. 2012; *6* Lake Donggi Cona, Mischke et al. 2010a; *7* Lake Kuhai, Mischke et al. 2010b; *8* Lake Koucha, Mischke et al. 2008). The bathymetric map of Lake Qinghai (modified from Colman et al. 2007): The *white squares* indicate the core site locations of QH07 (this study), LQDP05-2A, QH-2000, LQDP05-1Fs, and QH85-14B

of shorelines (Madsen et al. 2008; Liu et al. 2010, 2011, 2012; Rhode et al. 2010); the reason for the discrepancy is not yet fully understood.

Although the broad outlines of glacial-interglacial climate changes in East Asia and the differences in the timing of Holocene warmth on the Tibetan Plateau are generally known, the details are not well understood. Unresolved issues include the abruptness of the climate changes, the relative magnitude of millennial-scale fluctuations, and the interactions between the summer monsoon and lake basin responses on the Tibetan Plateau. We aim to address these questions

through multi-proxy investigations of Lake Qinghai sediments.

In this paper, we use broadly accepted terms such as the Bølling–Allerød and the Younger Dryas in a chronological sense to refer to the time intervals when these globally observed events occurred. We do not imply that the character or the causal mechanisms of the related climate changes in the Northern Atlantic area are the same as those in Central Asia.

Study site

Lake Qinghai, a closed basin at an elevation of 3,194 m, is situated at the northeastern margin of the Tibetan Plateau. The drainage area of the lake is about 30,000 km^2 (LZCAS 1994), from which five major rivers discharge to the lake basin. The Buha River, on the western side of the lake, contributes more than 60 % of the total runoff. Its drainage area is dominated by late Paleozoic sedimentary rocks (marine limestones and sandstones). Triassic volcanics and Mesozoic granodiorites are common in catchments of smaller tributaries (Yan et al. 2002; Yu and Zhang 2008). The surrounding mountain glaciers are generally small in size, from which the melt water only accounts for 0.3 % of the total inflow to the lake; thus, the influence of melt water on the water budget is relatively small. Although there is no surface outflow, groundwater through-flow may be substantial (Jin et al. 2010).

The lake has a surface area of 4,400 km^2, and an average water depth of 21 m, with a maximum depth of 27 m. It has three sub-basins: the northern, the southern, and the southeastern basins. Mean annual precipitation in this region is $\sim$360 mm, most of which falls in summer, while the potential evaporation is up to 1,000 mm per year at the lake surface. About 75 % of the total runoff occurs in the summer time. Annual mean temperature is -0.7 °C and monthly means exhibit remarkable seasonality, varying from -11 °C in winter to 12 °C in summer (Lister et al. 1991; Shen et al. 2005; Henderson et al. 2010).

The lake water is brackish (average salinity = 15.5 g L^{-1}; pH = 9), dominated by sodium, magnesium, potassium, chlorine, carbonate, and sulphate ions, mainly from weathering in the catchment of the Buha River, partly from atmospheric deposition (7.4–44 %), and only modestly from groundwater input (3.7–4.7 %; Jin et al. 2010). The lake is supersaturated with respect to carbonates including aragonite, calcite, and dolomite (Sun et al. 1991; Yu and Zhang 2008). High Mg/Ca (61–100) promotes aragonite precipitation directly from the lake water. The entire water column is oxic, but pore water becomes suboxic a few centimeters below the water/sediment interface.

Materials and methods

Sediment cores and sampling

As a complementary study to the Lake Qinghai Drilling Project (LQDP, An et al. 2006), a 355-cm-long Uwitec piston core (QH07-1A) and an 85-cm-long mini-Mackereth core (QH07-1B-1MM) were collected from a pontoon boat, at a water depth of 24.2 m, from the southeastern basin of Lake Qinghai, at LQDP site 2 (36°43′36.7″N, 100°29′28.1″E; Fig. 1). The top 15 cm of QH07-1B-1MM was soupy and was extruded and sampled at 0.5 cm intervals in the field. In the laboratory, discrete samples were taken continuously at 3-cm intervals from the Uwitec core and at 1.5-cm intervals from the mini-Mackereth core.

Dating methods

The age model for the composite record (QH07) was established on the basis of 17 AMS ^{14}C ages (5 ages from QH07-1B-1MM and 12 ages from QH07-1A; Electronic Supplementary Material). Two of the radiocarbon ages were from seed samples of the aquatic plant *Ruppiaceae*. The rest were determined on bulk organic matter because of the lack of terrestrial plant macrofossils in the sediments. A uniform reservoir correction of 700 years was applied to the radiocarbon ages before they were calibrated (Henderson and Holmes 2009; Henderson et al. 2010).

The radiocarbon ages were calibrated and an age model was generated using CLAM software ('classical' age-depth modeling) based on probability sampling methods that take into account multi-modal and asymmetric distributions of calibrated radiocarbon dates (Blaauw 2010). Five outliers are considered following the guidance of Bpeat software (Blaauw and Christen 2005). The smooth-spline method in CLAM was adopted for the age model with a smoothing level of 0.4.

The age modeling produced a 'best' age model (solid line in Fig. 2) as well as uncertainty ranges

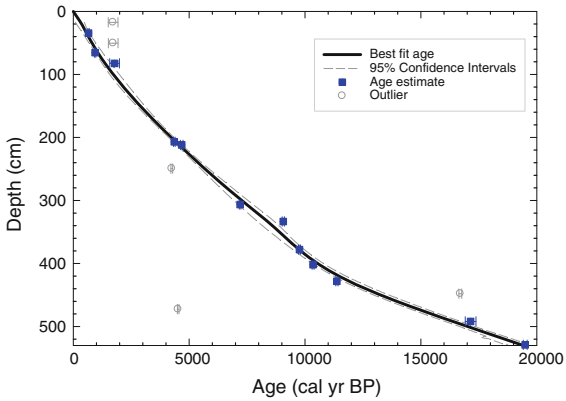

Fig. 2 Age-depth model for QH07 (in calibrated years BP) using a smooth spline model in CLAM (Blaauw 2010, smoothing factor, 0.4). *Dashed lines* show 95 % CI around the age model. *Solid line* shows the "best" fit of the age estimates. A modern age was assumed for the sediment surface and a constant 700-year reservoir effect was used in the age model

(95 % CI, dashed lines in Fig. 2), by finding the highest posterior probability density of the array of age-depth curves. Ages were weighted inversely with the error in their calibrated probabilities. Confidence intervals were calculated at the 2 standard deviation (95 %) level based on 10,000 iterations.

Based on field observations, the mini-Mackereth core sampled the undisturbed sediment–water interface. Comparison of magnetic susceptibility and elemental chemistry profiles among different cores at this site, including the nearby continuous drill core (LQDP05-2A), allows construction of a composite depth scale for the cores. These comparisons and the resulting composite depth scale indicate a gap between the mini-Mackereth and the Uwitec core, probably because of over-penetration by the latter. The size of the gap ($\sim$1 m) estimated from the susceptibility and chemistry profiles of the different cores is consistent with the radiocarbon analyses used to construct the composite age model (Electronic Supplementary Material).

Analytical methods

Magnetic susceptibility and bulk density analyses

Measurements of magnetic susceptibility at 1-cm intervals were performed on split cores using an automated core logger (Geotek MSCL-XYZ). The susceptibility reading was reported as volume-normalized susceptibility in units of 10^{-6} SI. In addition, the split cores were scanned using a Geotek MSCL-S to measure gamma-ray transmission, which provided an estimate of bulk density (g cm^{-3}), an indicator of lithology and porosity.

Bulk geochemical element analysis

Bulk elemental compositions of the sediments in split cores were analyzed using an ITRAX X-ray Fluorescence (XRF) Core Scanner (Cox Analytical Instruments). The measurements were taken at 2-mm intervals with a sampling time of 90 s using a molybdenum X-ray source set to 30 kV and 30 mA. Initial XRF spectral data were reprocessed in a standard fitting procedure using Q-Spec spectral analysis software to refine the individual elemental peak areas (Croudace et al. 2006). Final XRF results were reported as counts per second (cps), representing relative element concentrations. Measurements of incoherent and coherent scattering were produced during XRF scanning. Inc/coh can be used as a qualitative indicator of total organic matter concentrations because it depends on the average atomic number of material in the sediment (Burnett et al. 2011; Liu 2011), provided that the inorganic composition of sediments is relatively invariant.

Carbonate analysis

Total inorganic carbon in the sediments was measured by coulometry. Samples were freeze-dried and ground into fine, homogenous powder and desiccated overnight. Carbon dioxide gas evolved by reaction of carbonates in the sample with acid (30 mg sediment and 5 mL 2N HCl) was recorded as micrograms of carbon. Blanks and standards were run between every 10 samples. The amount of carbonate was calculated by assuming all inorganic carbon was present as calcium carbonate.

Analysis of TOC, TN and their isotopic ratios

Samples were freeze-dried, ground into fine powder, oven-dried at 60 °C overnight, and treated by acid fumigation (HCl) for 6 h to remove carbonate in the sediments. Fumigated samples wrapped in tin capsules were placed in a desiccator until EA-IRMS (Elemental Analysis-Isotope Ratio Mass Spectrometry) analyses. TOC and TN were reported as weight percentages.

Total organic matter (TOM) is estimated as 2×TOC. C/N weight ratios were converted to atomic ratios. Carbon and nitrogen isotopic ratios of the organic matter were determined by a Finnigan Delta Plus XP isotope-ratio mass spectrometer. The carbon isotope ratios were reported in δ values relative to the Vienna PeeDee Belemnite standard (VPDB), using the equation $\delta = [(R_{sample} - R_{standard})/R_{standard}] \times 1{,}000$. Nitrogen isotope ratios are reported in standard delta notation relative to air.

Grain size analysis

About 1 cm^3 wet bulk sediment was pretreated with 50 mL 30 % H_2O_2 and then with 20 mL 10 % HCl solution in a water bath (85 °C), to remove organic matter, carbonate, and iron oxides in sediments (Konert and Vandenberghe 1997). Then, 10 mL sodium hexametaphosphate solution (5 g L^{-1}) was used to disperse grains. Just before analysis, sample tubes were placed in a shaker bath and then analyzed on a Beckman Coulter LS 13 320 Particle Size Analyzer. Grain-size distribution was reported in 93 size classes between 0.375 and 2,000 μm.

Results

Chronology

Radiocarbon dating of bulk organic matter and *Ruppiaceae* seeds yielded ^{14}C ages between 1,390 ± 30 and 17,062 ± 83 year BP. The age model generated a reservoir-corrected age of 57 cal year BP for surface sediment of QH07-1B-1MM and provides a robust fit to the individual calibrated ages, particularly at the glacial/Holocene transition (11,500 cal year BP). The model indicates that our sedimentary record reaches back close to 20,000 cal year BP (Fig. 2). The sedimentation rates varied through the sequence, from a rate of ∼0.14 mm $year^{-1}$ during the late glacial period to about 0.37 mm $year^{-1}$ in the Holocene.

Analytical results

Sedimentological properties

Water content shows a sharp change at the late Pleistocene/Holocene transition, at ∼11,500 cal year BP, increasing from 20 to 50 % (Fig. 3). The density exhibits high values (∼2.3 g cm^{-3}) in glacial times and low values (∼1.7 g cm^{-3}) in the Holocene. Cl/Ti ratios derived from XRF measurements show high values before ∼11,500 cal year BP, and low values after that. The effects of compaction below ∼15 cm (upper watery sediments) seem relatively minor.

The carbonate content varies from about 20 to 60 % (by weight) throughout the core (Fig. 3). During the glacial period, carbonate content is low and remains relatively stable, fluctuating in a narrow range between 20 and 28 %. Early to middle Holocene sediments have relatively high concentrations with large variability (as low as 30 % and as high as 60 %, average ∼45 %). Late Holocene sediments contain ∼30 % carbonate. Ca/Ti profiles derived from XRF measurements show variations similar to carbonate content.

Organic geochemical measurements

TOC is low (∼0.6 %) and relatively constant during the glacial period (Fig. 4). An abrupt change occurs at ∼11,500 cal year BP, marked by relatively higher TOC (∼2 % on average, but up to 3 %). Inc/coh ratios from QH07 are relatively low during the glacial period and high in the Holocene. The TN profile shows values of ∼0.07 % during glacial times and ∼0.2 % in the Holocene. C/N ratios are relatively constant. The late Pleistocene shows lower C/N (<10) than does the Holocene (average about 12).

With respect to stable-isotope measurements of organic matter, $\delta^{13}C_{OM}$ values range from −28 to −20 ‰. During glacial times, $\delta^{13}C_{OM}$ varies slightly and averages ∼−24 ‰. It dramatically shifts to a more positive value (−20 ‰) in the early Holocene, gradually decreases to about −24 ‰ during the middle Holocene, and decreases to more negative values (∼−27 ‰) during the late Holocene. The $\delta^{15}N_{OM}$ falls in the range of +3 to +10 ‰, and it shows relatively constant values (∼5 ‰) during glacial times. The $\delta^{15}N_{OM}$ values are higher (∼7–8 ‰) in the Holocene.

Terrigenous sediment properties

Si/Ti values (Fig. 6) range from 0.1 to 0.3, and are relatively high during the glacial period, and relatively low in the Holocene. K/Ti ranges from 1 to 2.5 and

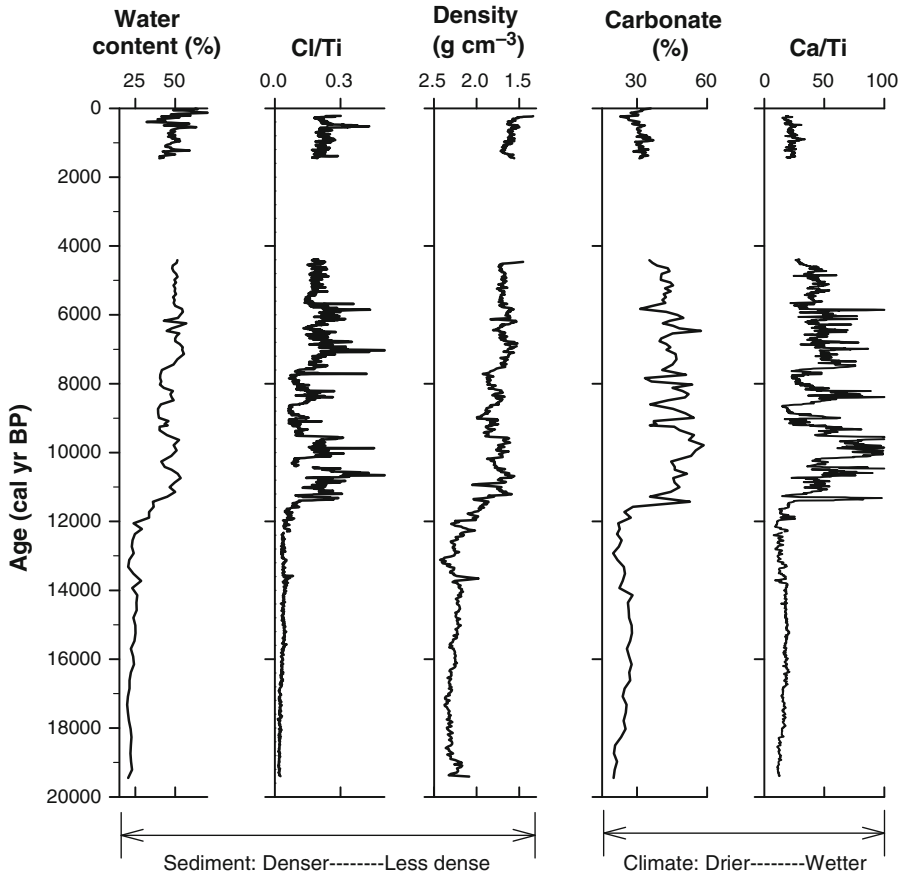

Fig. 3 Results from lithological and sedimentologic measurements, including water content, Cl/Ti from XRF (water content index), bulk density, carbonate content, and Ca/Ti from XRF (reflecting carbonate content)

shows the opposite trend. Typical Holocene-age sediment grain-size distributions have three major modes, centered at 9, 28, and 160 μm, and two minor modes, centered at 80 and 500 μm, whereas a typical glacial-age sediment grain-size distribution has only the three major modes seen in the Holocene. The mean grain-size profile shows similar trends as that for the content of the >116 μm fraction, being relatively coarse in the Holocene compared to earlier times. Magnetic susceptibility, iron, and titanium profiles from QH07 exhibit parallel changes, with high values in glacial times and low values in the Holocene.

Discussion

Age model

In this and in previous studies (Shen et al. 2005; Henderson et al. 2010; An et al. 2012), radiocarbon ages on *Ruppiaceae* seeds from Lake Qinghai are indistinguishable from those on bulk organic matter at the same horizon. *Ruppiaceae* seeds occur irregularly in the core, not in any concentrated pattern that might indicate shallow water. Previous studies have shown that the organic matter in the Lake Qinghai sediments is mainly aquatic (Shen et al. 2005; Yu and Zhang 2008), consistent with our measurements of radiocarbon ages of *Ruppiaceae* seeds compared to bulk organic matter. This implies that terrestrial organic matter input has a relatively small influence on bulk radiocarbon ages from Lake Qinghai.

Five outliers in the radiocarbon ages were identified, either because they created apparent age reversals, were far removed from regression fits, or were incompatible with multiple age estimates from other levels close by in the core. The reason for the outliers is not known, but in general, possible causes include contamination of samples by younger carbon, transport of carbon older than the sediments to the lake, and redeposition or slumping of previously deposited materials. The upper two outliers are particularly hard

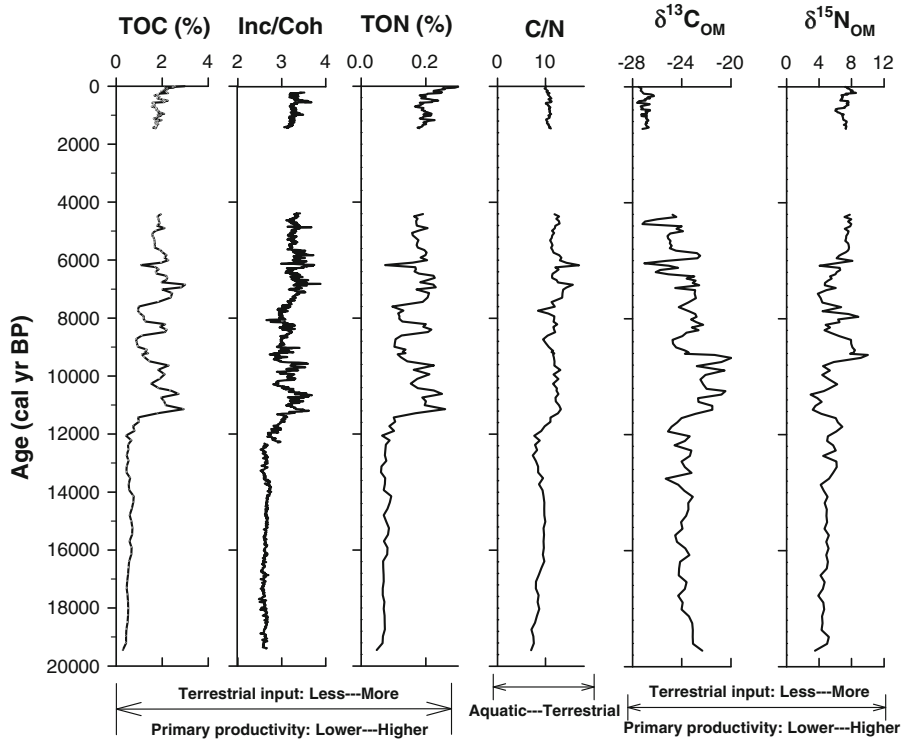

Fig. 4 Results from organic geochemical proxies, including total organic carbon, Inc/Coh ratio from XRF (reflecting total organic matter), total organic nitrogen, C/N, and the carbon and nitrogen isotopic composition of bulk organic matter ($\delta^{13}C_{OM}$ and $\delta^{15}N_{OM}$)

to explain except by laboratory contamination during sampling or processing, because there is no evidence of root penetration or major bioturbation at the relatively deep-water core site.

Radiocarbon ages of aquatic material at Lake Qinghai need to be corrected for lake reservoir effects, resulting from input of old inorganic carbon, dissolved by chemical weathering of carbonate rocks in the watershed, or contributed by terrestrial organic matter that has aged in the drainage basin before its final sequestration in the sediments. The issue of reservoir ages in lakes on the Tibetan Plateau is complex (Mischke et al. 2013), but previous estimates of the reservoir effect in Lake Qinghai range from 135 to 2,500 years (Shen et al. 2005; Yu et al. 2007; Henderson et al. 2010; Hou et al. 2010; An et al. 2012). In some cases (Henderson et al. 2010; An et al. 2012), estimates of the modern reservoir effect were partly derived from dated surface sediments, which may produce minimum ages because of the presence of "bomb" radiocarbon, derived from atmospheric testing of nuclear weapons in the 1960s and 1970s. Dating of terrestrial lignin phenols compared to TOC ages suggests that the reservoir effect may have varied between 750 and 1,500 years in the late Quaternary. These data and geochemical models (Yu et al. 2007) suggest that fluctuations in the magnitude of the reservoir effect as large as those suggested by An et al. (2012), 135–2,500 years, are unlikely.

Henderson et al. (2010) derived values for the modern reservoir effects using several methods. They obtained ^{14}C ages of 640, and 672 years for total organic carbon and authigenic carbonate, respectively, in surface sediment. They also obtained a ^{14}C age of 661 years for dissolved organic carbon in lake water. They derived a longer-term average estimate of the reservoir effect, 737 years, using a linear regression through ages at depth in their core, extrapolating that relation to the sediment surface. The consistency among these values suggests that a reservoir age of about 700 years is a good approximation of the modern reservoir effect. Finally, this value is consistent with age models and sedimentation rates derived from well-behaved ^{137}Cs and ^{210}Pb data (Henderson et al. 2010); a significantly larger modern reservoir effect would create a conflict in sedimentation rates derived from the ^{14}C and the ^{210}Pb data.

For the purposes of this paper, we take the conservative approach of using a modern reservoir effect of about 700 years, and assume that this value has not

varied with time. These are both oversimplifications, but we lack definitive evidence with which to construct alternate schemes. This 700-year value is consistent with extrapolation of our uncorrected radiocarbon data to the sediment surface (the corrected age model has a surface intercept of 57 years), suggesting no major change in reservoir effect in the recent past. Finally, what we interpret as the main change in environmental proxy measurements at the Pleistocene-Holocene boundary occurs in our cores at 11,500 cal year BP according to our age model. This is very close to estimates for the end of the Younger Dryas cool interval in many climate records, including the Chinese speleothems (Wang et al. 2001; Yuan et al. 2004), suggesting that a reservoir correction of approximately 700 years is appropriate at the time of the Pleistocene-Holocene transition.

Sedimentation rates (average $\sim$0.37 mm year^{-1}) in the Holocene derived from the age-depth model for QH07, are consistent with those for QH85-14B (from the south basin, Holocene sedimentation rate, 0.3–0.4 mm year^{-1}; Lister et al. 1991), QH-2000 (from the southeastern basin, Holocene sedimentation rate, 0.32–0.64 mm year^{-1}; Shen et al. 2005) and LQDP05-1Fs (from the south basin, Holocene sedimentation rate, 0.43 mm year^{-1}; An et al. 2012). Overall, the south basin cores have higher accumulation rates than those from the southeastern basin during the glacial time: $\sim$0.67 mm year^{-1} in LQDP05-1Fs and $\sim$0.5 mm year^{-1} in QH85-14B, versus 0.29–0.77 mm year^{-1} in QH-2000 and $\sim$0.14 mm year^{-1} in QH07.

Interpretation of individual paleoenvironmental indicators

The Cl/Ti ratios based on XRF measurements are related to the amount of pore water in the core, because most Cl is present as ions in pore water. Profiles of the Cl/Ti ratio in QH07 are consistent with water content and density measurements (Fig. 3). Increased water content, high Cl/Ti, and relatively low density, all reflect the increased porosity in Holocene sediments, which in turn implies a different bulk composition.

Carbonate minerals (primarily aragonite) are a major component of Lake Qinghai sediments, and the carbonate content of lake sediments is potentially controlled by several climate-related factors (Talbot and Kelts 1986). First, calcium carbonate precipitation can occur by evaporative concentration in lake water, which may cause the products of Ca^{2+} and CO_3^{2-} ion activities to exceed saturation. Under these conditions, high carbonate content implies relatively dry climate conditions. Second, the solubility of calcium carbonate decreases with increasing temperature, so that sediment carbonate content is enhanced by warm water. Third, photosynthesis and respiration can affect the equilibrium of the carbonate system through losses and gains of dissolved CO_2, respectively. High primary production in lake systems removes aqueous CO_2 in the process of photosynthesis, increasing pH and promoting carbonate precipitation. Fourth, if one of the ions, either the cation (Ca^{2+}) or the anion (CO_3^{2-}) is present in excess of saturation, the other becomes limiting to carbonate precipitation in the lake system. The addition of the limiting ion results in enhanced carbonate precipitation and rapid removal of the limiting ion.

The Ca^{2+} concentrations in modern Qinghai lake water are low ($\sim$11.0 ppm), compared to those in major input rivers ($\sim$58.8 ppm in Buha River; $\sim$69.6 ppm in Heima River; $\sim$56.8 ppm in Shaliu River). In contrast, total dissolved inorganic carbon concentration in the lake is relatively high ($\sim$291.0 ppm; Jin et al. 2010). Results from MINEQL+ 4.6 (Schecher and McAvoy 1992), show that the lake water is saturated with respect to calcite and nearly saturated with respect to aragonite. Moreover, carbonate content in recent sediments covaries with the observed water discharge of the Buha River, the largest input river for Lake Qinghai, for the last 50 years (An et al. 2012). Thus, it appears that the carbonate chemistry of the lake is calcium-limited, so that carbonate precipitation closely relates to Ca^{2+} delivered by river runoff, which in turn relates to precipitation in this region. The overall chemistry of the lake may have varied with temporal changes in evaporation rates, glacial meltwater runoff, or lake ice cover. Nevertheless, because of the strongly evaporative water balance of the area and because Lake Qinghai apparently was always a closed basin, the lake was likely Ca-limited for our entire record. Therefore, carbonate content (or the related Ca/Ti ratio) in Lake Qinghai sediments can be used as an indicator of river runoff. In this way, Lake Qinghai behaves much the same as Mono Lake, California, USA (Zimmerman et al. 2011), another closed, alkaline lake in a semi-arid environment.

Although we interpret runoff as the primary control (through calcium limitation) on carbonate sedimentation

in Qinghai Lake, other factors may have secondary effects. Changes in lake level may affect carbonate flux by delivery of river-borne clastic material (Zhao et al. 2010). Also, water temperature may have an effect, although given the likely amplitude of glacial-interglacial temperature change, the variation in calcium carbonate solubility is small compared to the change in carbonate content in Lake Qinghai sediments. Finally, although primary productivity in Lake Qinghai increased from the late Pleistocene to the Holocene, it remained relatively low even in the Holocene, as judged from TOC contents. Increased productivity and water temperature in the Holocene would have added to the effect of increased Ca^{2+} delivery to the lake in increased runoff.

Although organic carbon may be consumed by respiration or oxidation during early diagenesis, TOC content in sediments generally reflects lake primary productivity (including that by macrophytes) and the input of terrestrial organic matter. Both lacustrine production and terrestrial inputs are likely linked to increased precipitation and warm temperature, probably because freshwater input decreases lake water salinity and thereby enhances aquatic productivity (Henderson and Holmes 2009). Thus, we suggest that TOC, through complicated links between effective moisture and temperature and terrestrial and aquatic productivity, can be interpreted as an indicator of monsoonal strength at Lake Qinghai.

The C/N ratio of organic matter is extensively used as a source indicator of organic matter in terms of original proportions of aquatic and terrestrial material, despite diagenetic alteration (Meyers 1994). Algae have low C/N, typically in the range of 4–10, whereas land plants have C/N of 20 and greater (Meyers and Lallier-Verges 1999). Higher C/N suggests increased contribution of organic matter from land plant debris and/or aquatic macrophytes in the shallow parts of the lake. The results from QH07 suggest that organic matter deposited during glacial times was mainly from aquatic sources, whereas organic matter in the Holocene sediments was a mixture of aquatic and terrestrial material, but mostly aquatic.

The stable isotopic composition of bulk organic matter ($\delta^{13}C_{OM}$) in sediments is affected by the source material, fractionations during carbon assimilation, metabolism, and synthesis, and microbial reworking of organic matter during early diagenesis (Hayes 1993; Werne and Hollander 2004). $\delta^{13}C$ of land-derived organic matter depends on the photosynthetic pathway utilized: C_3, C_4 or CAM. The carbon isotope range of C_3 plants is −35 to −22 ‰, with a mean of ~−28 ‰; that of C_4 is −16 to −9 ‰, with a mean of ~−14 ‰. CAM plants have a large range of $\delta^{13}C$ that covers the range of the C_3 and C_4 pathways (DeNiro 1987; O'Leary 1988). $\delta^{13}C$ of aquatic organic matter is mainly affected by the $\delta^{13}C$ of the dissolved inorganic carbon ($\delta^{13}C_{DIC}$) in lake water because aquatic plants preferentially take up ^{12}C during photosynthesis, leaving the remaining dissolved inorganic carbon pool enriched in ^{13}C. Enhanced primary productivity thereby leads to a more positive $\delta^{13}C_{OM}$ (Meyers and Lallier-Verges 1999). However, carbon source, whether CO_2 (aq) or HCO_3^-, is also important because the two species have different fractionation factors.

Interpretation of the nitrogen isotopic composition of organic matter ($\delta^{15}N_{OM}$) is complex (Schulz and Zabel 2009). Similar to $\delta^{13}C_{OM}$, $\delta^{15}N$ of aquatic sources is thought to be associated with primary productivity (Meyers 1994). Despite complications in interpreting $\delta^{15}N_{OM}$, we suggest that low-frequency variations in $\delta^{15}N_{OM}$ reflect variation in aquatic production, whereas high-frequency variations imply changes in the relative proportion of terrestrial versus aquatic sources (Fig. 5e).

In general, all the organic geochemical measurements suggest low primary production in the lake during the glacial period, highest productivity in the early Holocene, and decreasing productivity into the late Holocene. These changes in lake primary productivity (phytoplankton or macrophytes) may be caused by variations in nutrient supply from the catchment, in addition to temperature and precipitation. TN shows a roughly linear relationship with TOC (Fig. 5a). The C/N ratio shows linear correlation with TOC and $\delta^{13}C_{OM}$ during glacial times, but not in the Holocene (Fig. 5b, d). A cross-plot of $\delta^{13}C_{OM}$ versus TOC (Fig. 5c) shows that the $\delta^{13}C_{OM}$ values in glacial sediments have a narrow range, whereas the $\delta^{13}C_{OM}$ data in Holocene sediments are rather scattered. We conclude that during glacial times, the $\delta^{13}C_{OM}$ not only reflects the $\delta^{13}C$ values of algae (C/N < 10, aquatic source), but also indicates low primary productivity. More positive values of $\delta^{13}C_{OM}$ in the early Holocene mostly indicate enhanced lake production. The variations of $\delta^{13}C_{OM}$ during the Holocene are likely caused by the introduction of a small, but variable proportion of terrestrial organic matter.

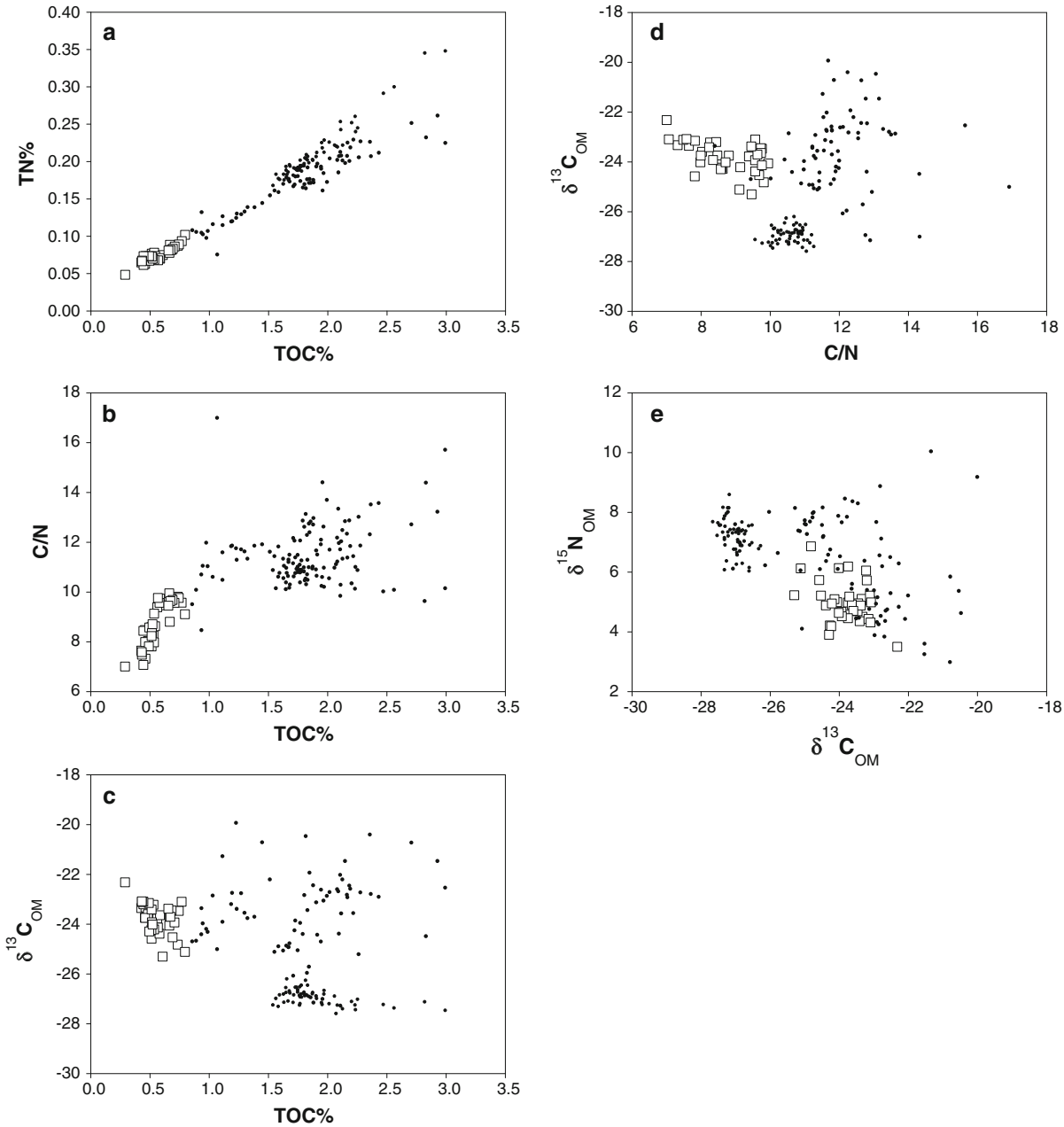

Fig. 5 Cross plots of **a** TOC versus TN; **b** TOC versus C/N; **c** TOC versus $\delta^{13}C_{OM}$; **d** C/N versus $\delta^{13}C_{OM}$; and **e** $\delta^{13}C_{OM}$ versus $\delta^{15}N_{OM}$. *Open squares* indicate data for the late Pleistocene and *solid dots* indicate data for the Holocene

The sources of the terrestrial organic matter during the early, middle, and late Holocene might have differed in response to vegetation change.

The magnetic susceptibility (Fig. 6) decrease in the early Holocene may be associated with the observed coarsening, if the coarser sediments are dominated by quartz instead of magnetically relevant minerals. In addition, authigenic carbonate also diluted the concentration of magnetic minerals during the Holocene.

The grain size of aeolian sediment has been used to reconstruct past variations of the Asian winter monsoon on the Loess Plateau (Porter and An 1995), in the

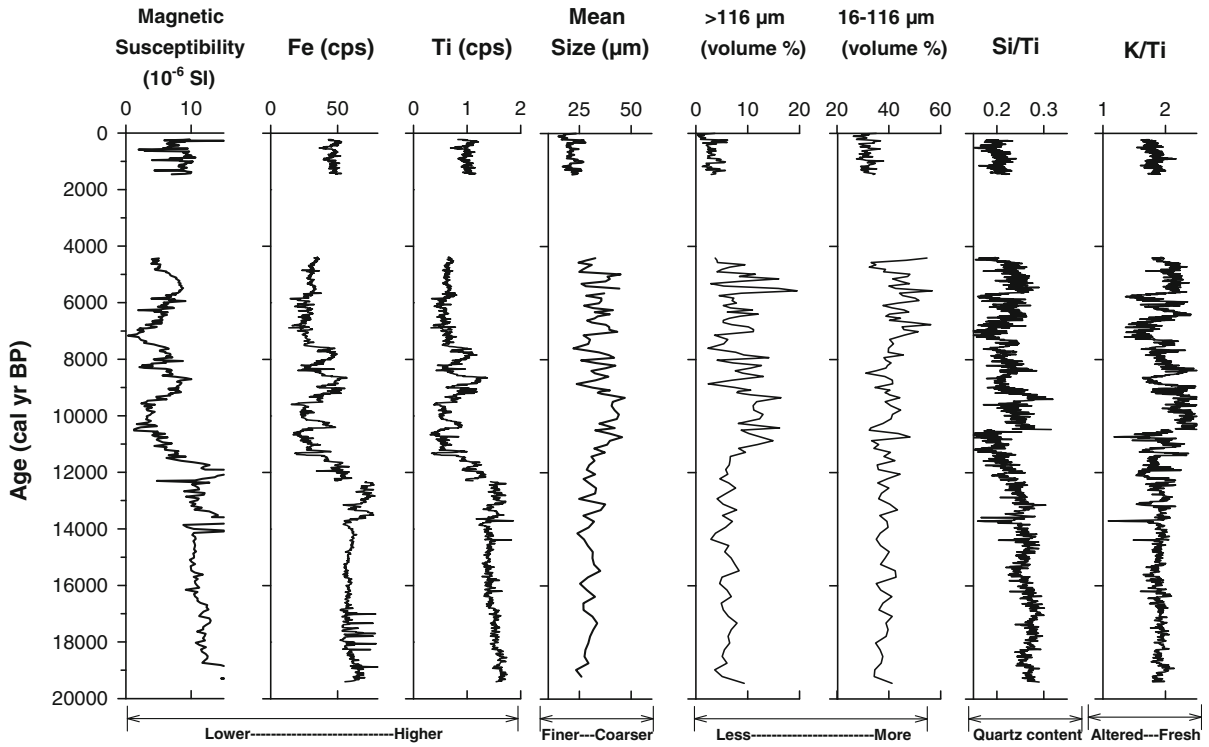

Fig. 6 Results for proxies derived from terrigenous sediment, including magnetic susceptibility, Fe content, Ti content, mean grain size, content of >116 μm fraction of lake sediment, content of 16–116 μm fraction, Si/Ti from XRF (index of quartz content), and K/Ti from XRF (index of weathering of the sediment)

North Pacific (Rea et al. 1998), and in Lake Biwa, Japan (Xiao et al. 1997). However, terrigenous sediment in most lakes is made up of materials from a combination of sources, including both aeolian and riverine load. Assuming there are multiple end members in terrigenous sediments, the aeolian component potentially can be separated from the riverine component.

An et al. (2012) suggested that the <25 μm fraction in Lake Qinghai sediments is derived mostly from riverine input, whereas the >25 μm fraction is primarily aeolian dust. This interpretation was based on observations of distinct grain-size characteristics in modern dust, loess, surface sediments, and riverine suspended particles. These results show high proportions of >25-μm sediments in glacial time and less coarse material during the Holocene, suggesting weakened westerlies in the Holocene (An et al. 2012).

However, the grain-size record from QH07, in the southeastern basin, appears quite different from that of LQDP05-1Fs, in the southern basin. Compared with LQDP05-1Fs, the coarse fraction (16–116 μm) in the size record from QH07 cores shows the opposite trend, i.e. higher contents of coarse fraction in the Holocene than in the glacial. Therefore, the coarse fraction in QH07 is difficult to interpret and cannot be simply explained as an aeolian signal.

The southeastern basin is shallower than the southern basin and QH07 is closer to the lake shore than LQDP05-1Fs. QH07 is also located offshore from the Erlangjian terrace, a hook-shaped sand spit prograding into the southeastern basin of Lake Qinghai. The coarse fraction in QH07 record may relate to local processes involving sand transport and progradation of the spit. The content of the >116-μm fraction (fine sand) in QH07 also increased during the Holocene compared to the late glacial. A decrease in the dust component in the early Holocene may partly explain the relative coarsening of detrital sediments in the Holocene.

Medium/coarse sand (500-μm-size) sporadically occurs in a few Holocene-age levels within the core. This seems anomalously coarse for this offshore site.

The sand may have been frozen into nearshore ice in the winter. During ice break-up, fragments may have rafted to offshore locations where ice melted and dropped the coarse sand. Another possibility is that the coarse sand was blown by winter winds onto the surface of the ice and was released offshore during spring melt and incorporated into the sediments, which are otherwise fine-grained.

Because quartz contains no Ti, if the Si/Ti ratio in other silicates is relatively constant, then the Si/Ti ratio of the bulk sediments likely reflects relative quartz content, i.e. high Si/Ti suggests high quartz content. K is mobilized more readily than Ti during chemical weathering, so sedimentary K/Ti reflects the degree of weathering of detrital sediment, i.e. high K/Ti suggests less-altered, fresher sediment sources. In QH07, intervals of high Si/Ti and low K/Ti during the glacial period are followed by episodes of low Si/Ti and high K/Ti during the Holocene, which suggests that less quartz and fresher silicates are present in Holocene sediments compared to glacial-age sediments. The greater Si/Ti and K/Ti variability may suggest multiple sediment sources.

Climate implications

Paleoclimate studies on the Tibetan Plateau have focused on various time scales (An 2000; Zhao et al. 2009; Chen et al. 2010). Chen et al. (2008) synthesized climate records from lake sediments at many sites in Central Asia. They found a distinct difference in moisture history during the Holocene between records from the northwest and the southeast parts of the Tibetan Plateau. The former showed a dry early Holocene, a less dry middle Holocene, and a moderately wet late Holocene, whereas the latter, monsoonal region showed a humid early Holocene and a relatively dry late Holocene (Chen et al. 2008). Herzschuh (2006) reconstructed moisture conditions in Central Asia during the last 50,000 years using 75 paleoclimate records. According to this synthesis, the middle and late marine isotope stage 3 was wet, whereas the last glacial maximum (LGM) was dry. Following the LGM, relatively wet climate conditions returned. Among the 75 records, most from the southeastern Tibetan Plateau show that the warmest, wettest Holocene climate conditions occurred during the early Holocene. Others, in northwest and north-central China and in Mongolia, however, show a middle Holocene, rather than the early Holocene temperature maximum. The majority of these paleoclimate records suggest reduced moisture since the middle Holocene (Herzschuh 2006).

The multiple variables we measured in the QH07 core from Lake Qinghai are compatible with each other and capture a distinct latest Pleistocene and Holocene climate record. The major first-order change in the record occurs at the transition between the latest Pleistocene and the Holocene, about 11,500 cal year BP, temporally correlative with the end of the Younger Dryas. The abruptness of the change might be explained by a sedimentary hiatus, and this possibility cannot be entirely eliminated. However, the available evidence argues against a significant hiatus. First, the abrupt change is independently observed in another (south) basin of the lake (An et al. 2012). Core sites in both basins are relatively deep, where hiatuses are less likely. Second, detailed sedimentological descriptions have not identified evidence for major unconformities. And finally, age models for this and others sites suggest no major hiatuses or missing sections in the accumulation of sediments.

Our interpretation that the carbonate content (also suggested by Ca/Ti) in Lake Qinghai sediments closely relates to river runoff allows us to use carbonate content as an indicator of the strength of the Asian summer monsoon, assuming a direct relation between precipitation and runoff. Another index of the summer monsoon strength is TOC, because TOC reflects lake primary productivity and/or the contribution of land-derived organic matter, probably both. In addition to percentages, we calculated the fluxes of carbonate and total organic matter, respectively.

The Asian summer monsoon is at least partly initiated by the differential heating between the Asian landmass and the Indian and Pacific Oceans (Li and Yanai 1996), although other processes may be involved (Molnar et al. 2010). Thus, the difference in June insolation between 30°N and 15°N (Huybers 2006), the approximate latitudes of Lake Qinghai and the South China Sea, respectively, is conceptually an index of this difference, so we compare it to the monsoon indicators in QH07.

The two summer monsoon indicators (Fig. 7) remain low and relatively constant during the glacial period ($\sim$20,000 to $\sim$14,600 cal year BP). During

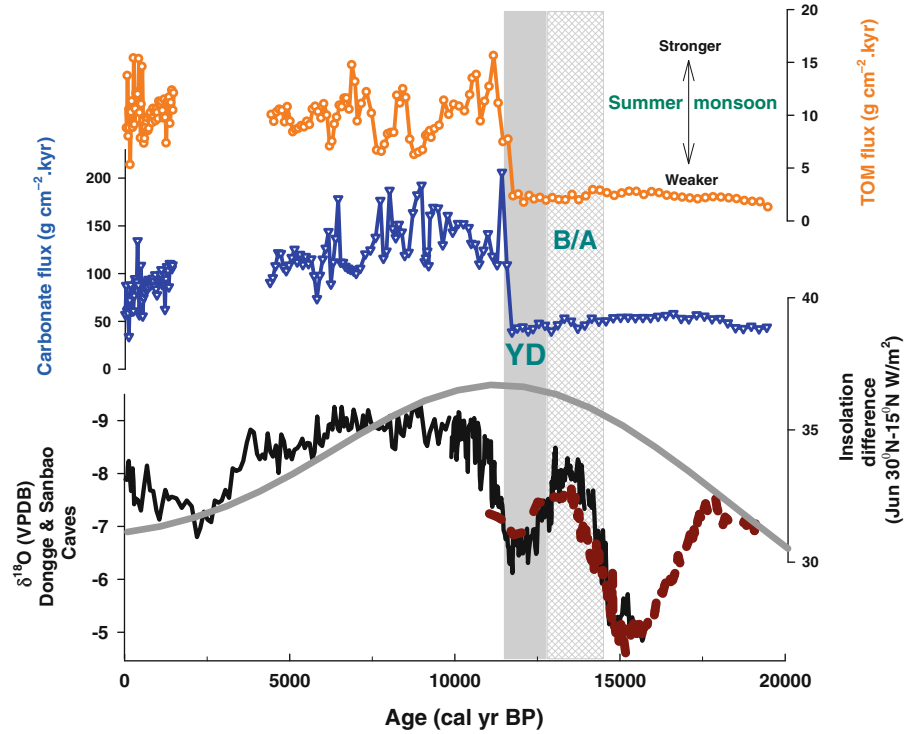

Fig. 7 Comparison of summer monsoon proxies for QH07 (*dotted orange line*: TOM flux; *solid blue line*: carbonate flux) with Dongge (*solid black line*) and Sanbao (*dashed red line*) cave speleothem δ^{18}O records and June insolation difference between 30°N and 15°N. *Gray bars* indicate the Bølling–Allerød (B/A) and Younger Dryas (YD) periods. (Color figure online)

the Holocene (~11,500 cal year BP to present), the indicators show higher values and greater variability in contrast to the glacial time. In the early Holocene (~11,500 to ~9,000 cal year BP), increase in organic matter and carbonate contents signifies the strongest summer monsoon, suggesting the occurrence of the warmest, wettest part of the Holocene, at the time of the insolation-difference maximum. Gradually reduced monsoonal precipitation (i.e. a weakened summer monsoon) since the middle Holocene is marked by a decrease in the carbonate and total organic matter content. The greater variability in the records of the Holocene implies complex, multiple sediment sources, but the overall trend follows that of insolation differences between 30°N and 15°N.

The QH07 record is consistent with what is known about the climate history in eastern China since the time of the Younger Dryas cold interval, i.e. wetter conditions in the early Holocene and drier conditions in the middle and late Holocene. The climate pattern broadly matches the insolation-difference record (Fig. 7), and implies that the orbitally induced difference in insolation is the major control on summer monsoon variability on glacial-interglacial timescales (Weber and Tuenter 2011). Feedbacks for the weakened summer monsoon during the glacial period may include lower sea level (more distant shoreline) and decreased continental albedo from increased snow and ice cover and vegetation change over Central Asia.

The QH07 record is quite consistent with other Qinghai core records (Fig. 1), such as QH85-14B (Lister et al. 1991), QH-2000 (Shen et al. 2005), LQDP05-1Fs (An et al. 2012) and LQDP05-2A (unpublished data). However, our interpretation of the QH07 record differs from that of recent studies of shoreline history at Lake Qinghai that used optically stimulated luminescence (OSL) age estimates (Liu et al. 2010, 2011, 2012). Those studies generated inferences for high stands of the lake during the Bølling–Allerød and middle Holocene, but do not identify a high lake-level stand during the early Holocene. The reasons for the difference between the interpretations derived from cores and from shoreline deposits are unknown, but might result from inherent chronological uncertainties in OSL and ^{14}C dating methods.

Several other paleoclimate records (Fig. 1) from the northeastern Tibetan Plateau show variable levels of consistency with our conclusions based on QH07. Many agree with a warm and/or wet maximum in the early Holocene. For instance, vegetation history inferred from pollen at Hurleg Lake suggests a moist

early Holocene (~11,900 to ~9,500 cal year BP) and a drying trend during the middle and late Holocene (Zhao et al. 2007). Studies of Lake Kuhai and paleolake Dalianhai also imply an early/middle Holocene optimum (Chen et al. 2010; Mischke et al. 2010b). In contrast, records from the Shiyang River drainage basin suggest a middle Holocene high stand (Li et al. 2012). Studies in the northern Ulan Buh Desert document a large paleolake during the interval 7,800–7,100 cal year BP, and show that this paleolake began to shrink and modern desert evolved during the late Holocene (Zhao et al. 2012). Some studies led to inferences for high lake levels during the late Holocene. For example, data from Lake Donggi Cona suggest relatively low lake level (brackish lake) during the late glacial and early/middle Holocene, and a relatively high lake level (freshwater lake) after 6,800 cal year BP (Mischke et al. 2010a). The Lake Koucha record shows a low lake level from 16,000 to 7,300 cal year BP and a gradual lake rise afterwards (Mischke et al. 2008). Most of these records do not show major Bølling–Allerød/Younger Dryas oscillations. However, the Chaka Salt Lake record from the eastern Qaidam Basin reveals distinct Bølling–Allerød/Younger Dryas changes, as well as a high lake level between 17,200 and 11,400 cal year BP, an abrupt transition from high to low lake level at the beginning of the Holocene, and a progressive decrease in level into the late Holocene (Liu et al. 2008). The differences among all these records suggest either problems in interpreting regional responses to climate change, or non-uniform responses of individual lakes because of local environmental factors. Chronological uncertainties, including the assumption of constant reservoir effects, may also play a major role.

Larger lakes are less sensitive to local climate perturbations and thus may be more likely to record regional climate information.

The QH07 record is remarkably similar to the Chinese speleothem records (Wang et al. 2001; Yuan et al. 2004), although some differences in detail are apparent. The Dongge and Sanbao cave records (Fig. 7) show major changes during the late glacial, such as those during the time of the Bølling–Allerød oscillation, whereas the QH07 record suggests that largely glacial conditions persisted from the LGM to the end of the Younger Dryas interval (~11,500 cal year BP). There is little or no evidence for a distinct change in conditions during the time of the Bølling–Allerød oscillation (~14,600–12,900 cal year BP), especially in the TOC and carbonate values. The cave records suggest a relatively gradual Younger Dryas/Holocene transition, whereas the equivalent change in QH07 is abrupt. Moreover, the cave records show lower variability during the Holocene than does QH07. These differences between QH07 and the Chinese cave records may be related to the fact that Lake Qinghai is further inland and at higher elevation than the Dongge and Sanbao caves. These contrasts also suggest the existence of a threshold for the arrival of monsoonal precipitation at Qinghai—a threshold that was crossed at the beginning of the Holocene. Because of the high elevation of the Tibetan Plateau, this may be related simply to the barrier that the plateau front poses to penetration of the summer monsoon into the continental interior, or it may relate to complex changes (such as the path of the westerly jet stream) within the climate system.

Conclusions

A multi-proxy approach was applied to the paleoenvironmental interpretations from the sediments in Lake Qinghai. Taken together, the results reveal climate variations, especially fluctuations in the strength of the Asian summer monsoon, as expressed in the properties of the sediments.

- Summer monsoon circulation was relatively weak and stable during the entire LGM and late glacial time, resulting in relatively cold, dry, and stable climatic conditions in the Qinghai region. In contrast, during the Holocene, the summer monsoon was stronger and showed enhanced variability, implying relatively wetter and less stable climatic conditions than during the late Pleistocene. The strongest summer monsoon, marked by increased organic matter and carbonate contents, occurred in the earliest Holocene and was followed by a drying trend during the middle and late Holocene.
- Near-glacial conditions persisted from the LGM to the end of the Younger Dryas interval. Little or no evidence of significant climate change during the equivalent to the Bølling–Allerød oscillation is revealed in the QH07 record.
- All of the paleoenvironmental indicators abruptly change across the Late-Pleistocene/Holocene transition, about 11,500 cal year BP. This change

appears to be more abrupt than the isotopic changes at the corresponding time in the Chinese speleothems.

- By comparing our Lake Qinghai record QH07 with the Northern Hemisphere insolation-difference record (between June 30°N and June 15°N), we propose that the changes in insolation contrast between the continent and the ocean is the major control on the Asian monsoon system over the glacial/interglacial time scales. Secondary influences may include albedo effects caused by changing ice cover and vegetation over central Asia and sea level (distance from moisture source in Pacific Ocean).
- Differences between the Lake Qinghai record and those from most Chinese speleothems suggest that a climate threshold existed for arrival of monsoonal rainfall on the northeastern Tibetan Plateau, and that this threshold was crossed at the beginning of the Holocene.

Understanding of the monsoon history of the Tibetan Plateau from lake sediments can be improved by additional research that provides more robust age models and novel proxies for both paleoprecipitation and paleotemperature. Separation of temperature and precipitation effects would be especially useful for evaluating the degree of association between warm and wet conditions. The interaction between the Tibetan Plateau and the atmosphere is key to understanding Asian monsoon variability and its climate controls. Interdisciplinary efforts by paleoclimatologists, geophysicists, and atmospheric scientists would be particularly useful.

Acknowledgments This work was supported by National Science Foundation grant EAR-0602412 to SMC. In addition, some AMS ^{14}C data were supported by a NERC-RCL allocation (1247.1007) to JAH and ACGH. We thank LacCore (National Lacustrine Core Facility), Limnological Research Center, University of Minnesota-Twin Cities for laboratory assistance. We also thank MOE Key Laboratory of Western China's Environmental Systems, Lanzhou University for field assistance. Helpful reviews were provided by David Madsen, Steffen Mischke, Mark Brenner, and an anonymous reviewer.

References

An ZS (2000) The history and variability of the East Asian paleomonsoon climate. Quat Sci Rev 19:171–187

An ZS, Wang P, Shen J, Zhang YX, Zhang PZ, Wang SM, Li XQ, Sun QL, Song YG, Al L, Zhang YC, Jiang SR, Liu XQ, Wang Y (2006) Geophysical survey on the tectonic and sediment distribution of Qinghai Lake basin. Sci China Ser D 49:851–861

An ZS, Colman SM, Zhou WJ, Li XQ, Brown ET, Jull AJT, Cai YJ, Huang YS, Lu XF, Chang H, Song YG, Sun YB, Xu H, Liu WG, Jin ZD, Liu XD, Cheng P, Liu Y, Ai L, Li XZ, Liu XJ, Yan LB, Shi ZG, Wang XL, Wu F, Qiang XK, Dong JB, Lu FY, Xu XW (2012) Interplay between the Westerlies and Asian summer monsoon recorded in Lake Qinghai sediments since 32 ka. Sci Rep 2:619–622

Blaauw M (2010) Methods and code for 'classical' age-modelling of radiocarbon sequences. Quat Geochronol 5:512–518

Blaauw M, Christen JA (2005) Radiocarbon peat chronologies and environmental change. J Roy Stat Soc: Ser C (Appl Stat) 54:805–816

Boos WR, Kuang Z (2010) Dominant control of the South Asian monsoon by orographic insulation versus plateau heating. Nature 463:218–222

Burnett AP, Soreghan MJ, Scholz CA, Brown ET (2011) Tropical East African climate change and its relation to global climate: a record from Lake Tanganyika, Tropical East Africa, over the past 90 + kyr. Palaeogeogr Palaeoclimatol Palaeoecol 303:155–167

Chen FH, Yu ZC, Yang ML, Ito E, Wang SM, Madsen DB, Huang XZ, Zhao Y, Sato T, Birks HJB, Boomer I, Chen JH, An CB, Wünnemann B (2008) Holocene moisture evolution in arid central Asia and its out-of-phase relationship with Asian monsoon history. Quat Sci Rev 27:351–364

Chen FH, Chen JH, Holmes J, Boomer I, Austin P, Gates JB, Wang NL, Brooks SJ, Zhang JW (2010) Moisture changes over the last millennium in arid central Asia: a review, synthesis and comparison with monsoon region. Quat Sci Rev 29:1055–1068

Chen FH, Zhang JW, Cheng B, Yang TB (2012) Late quaternary high lake levels and environmental changes since last deglacial in Da Lian Hai, Gonghe Basin in Qinghai Province. Quat Sci 32:122–131 (in Chinese with English abstract)

Colman SM, Yu SY, An Z, Shen J, Henderson ACG (2007) Late Cenozoic climate changes in China's western interior: a review of research on Lake Qinghai and comparison with other records. Quat Sci Rev 26:2281–2300

Croudace IW, Rindby A, Rothwell RG (2006) ITRAX: description and evaluation of a new multi-function X-ray core scanner. In: Rothwell RG (ed) New techniques in sediment core analysis, London, Geological Society, Special Publications, vol 267, pp 51–63

DeNiro M (1987) Stable isotopy and archaeology. Am Sci 75:182–191

Hayes JM (1993) Factors controlling ^{13}C contents of sedimentary organic-compounds—principles and evidence. Mar Geol 113:111–125

Henderson ACG, Holmes JA (2009) Palaeolimnological evidence for environmental change over the past millennium from Lake Qinghai sediments: a review and future research prospective. Quat Int 194:134–147

Henderson ACG, Holmes JA, Leng MJ (2010) Late Holocene isotope hydrology of Lake Qinghai, NE Tibetan Plateau: effective moisture variability and atmospheric circulation changes. Quat Sci Rev 29:2215–2223

Herzschuh U (2006) Palaeo-moisture evolution in monsoonal Central Asia during the last 50,000 years. Quat Sci Rev 25:163–178

Hou JZ, Huang YS, Brodsky C, Alexandre MR, McNichol AP, King JW, Hu FS, Shen J (2010) Radiocarbon dating of individual lignin phenols: a new approach for establishing chronology of Late Quaternary lake sediments. Anal Chem 82:7119–7126

Huybers P (2006) Early Pleistocene glacial cycles and the integrated summer insolation forcing. Science 313:508–511

Jin ZD, You CF, Wang Y, Shi YW (2010) Hydrological and solute budgets of Lake Qinghai, the largest lake on the Tibetan Plateau. Quat Int 218:151–156

Konert M, Vandenberghe J (1997) Comparison of laser grain size analysis with pipette and sieve analysis: a solution for the underestimation of the clay fraction. Sedimentology 44:523–535

Kutzbach JE, Guetter PJ, Ruddiman WF, Prell WL (1989) Sensitivity of climate to Late Cenozoic uplift in southern Asia and the American west—numerical experiments. J Geophys Res Atmos 94:18393–18407

Li CF, Yanai M (1996) The onset and interannual variability of the Asian summer monsoon in relation to land sea thermal contrast. J Clim 9:358–375

Li Y, Wang N, Li Z, Zhang H (2012) Basin-wide Holocene environmental changes in the marginal area of the Asian monsoon, northwest China. Environ Earth Sci 65:203–212

Lister GS, Kelts K, Zao CK, Yu JQ, Niessen F (1991) Lake Qinghai, China—closed-basin lake levels and the oxygen isotope record for ostracoda since the Latest Pleistocene. Palaeogeogr Palaeoclimatol Palaeoecol 84:141–162

Liu XJ (2011) Late Quaternary climate history on the northeast Tibetan Plateau: multi-proxy investigation of Lake Qinghai sediments, China. PhD dissertation, University of Minnesota

Liu X, Dong H, Rech JA, Matsumoto R, Bo Y, Wang Y (2008) Evolution of Chaka Salt Lake in NW China in response to climatic change during the Latest Pleistocene-Holocene. Quat Sci Rev 27:867–879

Liu X, Lai Z, Fan Q, Long H, Sun Y (2010) Timing for high lake levels of Qinghai Lake in the Qinghai-Tibetan Plateau since the Last Interglaciation based on quartz OSL dating. Quat Geochronol 5:218–222

Liu X, Lai Z, Madsen D, Yu L, Liu K, Zhang J (2011) Lake level variations of Qinghai Lake in northeastern Qinghai-Tibetan Plateau since 3.7 ka based on OSL dating. Quat Int 236:57–64

Liu X, Lai Z, Yua L, Sun Y, Madsen DB (2012) Luminescence chronology of aeolian deposits from the Qinghai Lake area in the Northeastern Qinghai-Tibetan Plateau and its palaeoenvironmental implications. Quat Geochronol 10:37–43

LZCAS (1994) (Lanzhou branch of Chinese Academy of Sciences) Evolution of recent environments in Qinghai Lake and its prediction. West Center of Resource and Environment, Chinese Academy of Sciences, Science Press, Beijing (in Chinese with English abstract)

Madsen DB, Ma H, Rhode D, Brantingham PJ, Forman SL (2008) Age constraints on the late Quaternary evolution of Qinghai Lake, Tibetan Plateau. Quat Res 69:316–325

Meyers PA (1994) Preservation of elemental and isotopic source identification of sedimentary organic-matter. Chem Geol 114:289–302

Meyers PA, Lallier-Verges E (1999) Lacustrine sedimentary organic matter records of Late Quaternary paleoclimates. J Paleolimnol 21:345–372

Mischke S, Kramer M, Zhang CJ, Shang HM, Herzschuh U, Erzinger J (2008) Reduced early Holocene moisture availability in the Bayan Har Mountains, northeastern Tibetan Plateau, inferred from a multi-proxy lake record. Palaeogeogr Palaeoclimatol Palaeoecol 267:59–76

Mischke S, Aichner B, Diekmann B, Herzschuh U, Plessen B, Wünnemann B, Zhang CJ (2010a) Ostracods and stable isotopes of a late glacial and Holocene lake record from the NE Tibetan Plateau. Chem Geol 276:95–103

Mischke S, Zhang CJ, Börner A, Herzschuh U (2010b) Late-glacial and Holocene variation in aeolian sediment flux over the northeastern Tibetan Plateau recorded by laminated sediments of a saline meromictic lake. J Quat Sci 25:162–177

Mischke S, Weynell M, Zhang C, Wiechert U (2013) Spatial variability of ^{14}C reservoir effects in Tibetan Plateau lakes. Quat Int. doi:10.1016/j.quaint.2013.01.030

Molnar P, Boos WR, Battisti DS (2010) Orographic controls on climate and paleoclimate of Asia: thermal and mechanical roles for the Tibetan Plateau. In: Jeanloz R, Freeman KH (eds) Annu Rev Earth Planet Sci, pp 77–102

O'Leary MH (1988) Carbon isotopes in photosynthesis. Bioscience 38:328–336

Pausata FSR, Battisti DS, Nisancioglu KH, Bitz CM (2011) Chinese stalagmite $\delta^{18}O$ controlled by changes in the Indian monsoon during a simulated Heinrich event. Nat Geosci 4:474–480

Porter SC, An ZS (1995) Correlation between climate events in the north-Atlantic and China during Last Glaciation. Nature 375:305–308

Rea DK, Snoeckx H, Joseph LH (1998) Late Cenozoic eolian deposition in the North Pacific: Asian drying, Tibetan uplift, and cooling of the northern hemisphere. Paleoceanography 13:215–224

Rhode D, Ma H, Madsen DB, Brantingham PJ, Forman SL, Olsen JW (2010) Paleoenvironmental and archaeological investigations at Qinghai Lake, western China: geomorphic and chronometric evidence of lake level history. Quat Int 218:29–44

Schecher WD, McAvoy DC (1992) MINEQL+: a software environment for chemical-equilibrium modeling. Comput Environ Urban Syst 16:65–76

Schulz HD, Zabel M (2009) Marine geochemistry. Springer, Berlin

Shen J, Liu XQ, Wang SM, Matsumoto R (2005) Palaeoclimatic changes in the Qinghai Lake area during the last 18,000 years. Quat Int 136:131–140

Sun DP, Tang Y, Xu Z, Han Z (1991) A preliminary investigation on chemical evolution of the Lake Qinghai water. Chin Sci Bull 36:1172–1174 (in Chinese with English abstract)

Talbot MR, Kelts K (1986) Primary and diagenetic carbonates in the anoxic sediments of Lake Bosumtwi, Ghana. Geology 14:912–916

Wang YJ, Cheng H, Edwards RL, An ZS, Wu JY, Shen CC, Dorale JA (2001) A high-resolution absolute-dated Late Pleistocene monsoon record from Hulu Cave, China. Science 294:2345–2348

Wang YJ, Cheng H, Edwards RL, Kong XG, Shao XH, Chen ST, Wu JY, Jiang XY, Wang XF, An ZS (2008)

Millennial- and orbital-scale changes in the East Asian monsoon over the past 224,000 years. Nature 451: 1090–1093

Weber SL, Tuenter E (2011) The impact of varying ice sheets and greenhouse gases on the intensity and timing of boreal summer monsoons. Quat Sci Rev 30:469–479

Werne JP, Hollander DJ (2004) Balancing supply and demand: controls on carbon isotope fractionation in the Cariaco Basin (Venezuela) Younger Dryas to present. Mar Chem 92:275–293

Xiao JL, Inouchi Y, Kumai H, Yoshikawa S, Kondo Y, Liu TS, An ZS (1997) Eolian quartz flux to Lake Biwa, central Japan, over the past 145,000 years. Quat Res 48:48–57

Yan JP, Hinderer M, Einsele G (2002) Geochemical evolution of closed-basin lakes: general model and application to Lakes Qinghai and Turkana. Sediment Geol 148:105–122

Yu JQ, Zhang L (2008) Lake Qinghai-paleoenvironment and paleoclimate. Science Press, Beijing

Yu SY, Shen J, Colman SM (2007) Modelling the radiocarbon reservoir effect in lacustrine system. Radiocarbon 49: 1241–1254

Yuan DX, Cheng H, Edwards RL, Dykoski CA, Kelly MJ, Zhang ML, Qing JM, Lin YS, Wang YJ, Wu JY, Dorale JA, An ZS, Cai YJ (2004) Timing, duration, and transitions of the Last Interglacial Asian Monsoon. Science 304:575–578

Zhao Y, Yu ZC, Chen FH, Ito E, Zhao C (2007) Holocene vegetation and climate history at Hurleg Lake in the Qaidam Basin, northwest China. Rev Palaeobot Palynol 145: 275–288

Zhao Y, Yu ZC, Chen FH, Zhang JW, Yang B (2009) Vegetation response to Holocene climate change in monsoon-influenced region of China. Earth-Sci Rev 97:242–256

Zhao C, Yu Z, Zhao Y, Ito E, Kodama KP, Chen F (2010) Holocene millennial-scale climate variations documented by multiple lake-level proxies in sediment cores from Hurleg Lake, Northwest China. J Paleolimnol 44:995–1008

Zhao H, Li GQ, Sheng YW, Jin M, Chen FH (2012) Early-middle Holocene lake-desert evolution in northern Ulan Buh Desert, China. Palaeogeogr Palaeoclimatol Palaeoecol 331:31–38

Zimmerman SRH, Hemming SR, Hemming NG, Tomascak PB, Pearl C (2011) High-resolution chemostratigraphic record of late Pleistocene lake-level variability, Mono Lake, California. Geol Soc Am Bull 123:2320–2334